

# A model for the interaction between NF-kappa-B and ASPP2 suggests an I-kappa-B-like binding mechanism

Hadar Benyamini,<sup>1</sup> Hadas Leonov,<sup>2</sup> Shahar Rotem,<sup>1</sup> Chen Katz,<sup>1</sup> Isaiah T. Arkin,<sup>2</sup> and Assaf Friedler<sup>1\*</sup>

<sup>1</sup>The Institute of Chemistry, The Hebrew University of Jerusalem, Givat Ram, Jerusalem 91904, Israel

<sup>2</sup>Department of Biological Chemistry, The Hebrew University of Jerusalem, Givat Ram, Jerusalem 91904, Israel

## ABSTRACT

We used computational methods to study the interaction between two key proteins in apoptosis regulation: the transcription factor NF- $\kappa$ -B (NF $\kappa$ B) and the proapoptotic protein ASPP2. The C-terminus of ASPP2 contains ankyrin repeats and SH3 domains (ASPP2<sub>ANK-SH3</sub>) that mediate interactions with numerous apoptosis-related proteins, including the p65 subunit of NF $\kappa$ B (NF $\kappa$ B<sub>p65</sub>). Using peptide-based methods, we have recently identified the interaction sites between NF $\kappa$ B<sub>p65</sub> and ASPP2<sub>ANK-SH3</sub> (Rotem *et al.*, *J Biol Chem* 283, 18990–18999). Here we conducted a computational study of protein docking and molecular dynamics to obtain a structural model of the complex between the full length proteins and propose a mechanism for the interaction. We found that ASPP2<sub>ANK-SH3</sub> binds two sites in NF $\kappa$ B<sub>p65</sub>, at residues 236–253 and 293–313 that contain the nuclear localization signal (NLS). These sites also mediate the binding of NF $\kappa$ B to its natural inhibitor I $\kappa$ B, which also contains ankyrin repeats. Alignment of the ankyrin repeats of ASPP2<sub>ANK-SH3</sub> and I $\kappa$ B revealed that both proteins share highly similar interfaces at their binding sites to NF $\kappa$ B. Protein docking of ASPP2<sub>ANK-SH3</sub> and NF $\kappa$ B<sub>p65</sub>, as well as molecular dynamics simulations of the proteins, provided structural models of the complex that are energetically similar to the NF $\kappa$ B-I $\kappa$ B determined structure. Our results show that ASPP2<sub>ANK-SH3</sub> binds NF $\kappa$ B<sub>p65</sub> in a similar manner to its natural inhibitor I $\kappa$ B, suggesting a possible novel role for ASPP2 as an NF $\kappa$ B inhibitor.

Proteins 2009; 77:602–611.  
© 2009 Wiley-Liss, Inc.

**Key words:** apoptosis; docking; molecular dynamics; peptides; ASPP2; NF $\kappa$ B; p53.

## INTRODUCTION

Programmed cell death (apoptosis) is regulated by complex protein interaction networks. The proapoptotic protein ASPP2 is a 1128 amino acids (AA) protein that is emerging as a hub of apoptosis regulation. The C-terminal part of ASPP2 was first discovered as p53-binding protein 2 (53BP2, ASPP2 AA 600–1128, Fig. 1<sup>1</sup>). Another truncated form of ASPP2 was isolated as a Bcl-2 binding protein (Bbp, ASPP2 AA 123–1128, Fig. 1<sup>2</sup>). In 2001, the full length ASPP2 was identified as a protein that specifically stimulates p53-dependent apoptosis.<sup>3</sup> The domain structure of ASPP2 includes an N-terminal ubiquitin-like domain,<sup>4</sup> followed by a predicted alpha helical domain and a proline-rich domain.<sup>5</sup> The ~200 C-terminal residues of ASPP2 consist of four ankyrin repeats followed by an SH3 domain (ASPP2<sub>ANK-SH3</sub>, Fig. 1<sup>6</sup>). ASPP2<sub>ANK-SH3</sub> mediates the protein-protein interactions of ASPP2. It interacts with numerous proteins, most of which are involved in apoptosis regulation, including p53 and its family members,<sup>3,7</sup> the antiapoptotic protein Bcl-2 family members,<sup>2,8</sup> protein phosphatase 1,<sup>9</sup> yes-associated protein,<sup>10</sup> hepatitis C virus core protein<sup>11</sup> and the p65 subunit of the transcription factor NF $\kappa$ B (NF $\kappa$ B<sub>p65</sub>).<sup>12</sup>

NF $\kappa$ B is a transcription factor involved in apoptosis regulation. The larger NF $\kappa$ B family contains two sub-families: “Rel” and “NF $\kappa$ B.”<sup>13</sup> Members of the two sub-families form homo- and hetero-dimers. The Rel proteins contain C-terminal transactivation domains (see Fig. 1). NF $\kappa$ B subfamily members have long C-terminal domains containing multiple copies of ankyrin repeats, which act to auto-inhibit these proteins. NF $\kappa$ B proteins are cleaved to form shorter proteins (p105 to p50 and p100 to p52), which bind DNA only when they form dimers with members of the Rel subfamily. The most abundant heterodimer is the p50/p65. The activity of NF $\kappa$ B is tightly regulated by an interaction with its natural inhibitor protein I $\kappa$ B. In most cells NF $\kappa$ B is in an inactive state, bound to I $\kappa$ B in the cytoplasm and its nuclear localization signal (NLS) is masked by I $\kappa$ B. Following a wide array of

Grant sponsors: Human Frontier Science Program Organization, Israel Cancer Association, Lady Davis Fellowship Trust.

\*Correspondence to: Assaf Friedler, The Institute of Chemistry, The Hebrew University of Jerusalem, Safra Campus, Givat Ram, Jerusalem 91904, Israel. E-mail: assaf@chem.huji.ac.il

Received 12 February 2009; Revised 7 April 2009; Accepted 27 April 2009

Published online 11 May 2009 in Wiley InterScience (www.interscience.wiley.com).

DOI: 10.1002/prot.22473

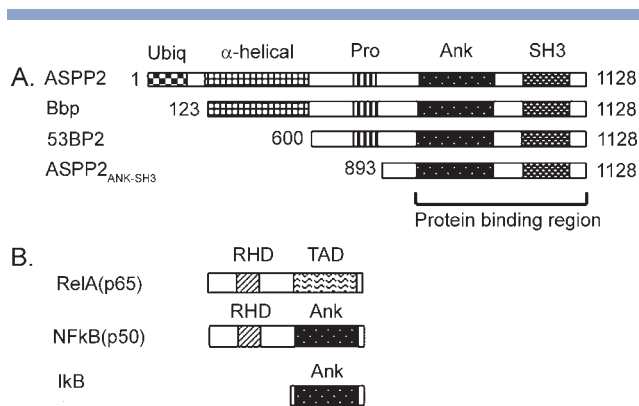


**Figure 1**

Domain organization of ASPP2 and its variants, and of NFκB and IκB. **A:** ASPP2 is the full length protein containing 1128 AA. It has a ubiquitin-like domain,<sup>4</sup> a predicted α-helical domain, a proline-rich domain, and a C-terminal protein binding region. The C terminal part contains the ankyrin-repeats domain and the SH3 domain. **B:** The domain structures of the Rel and NFκB subfamilies of the NFκB transcription factors, and IκB. All NFκB proteins have a conserved DNA-binding/dimerization domain called the Rel homology domain (RHD), which also has sequences important for nuclear localization and IκB binding. The C-terminal halves of the Rel proteins have transcriptional activation domains (TAD). The C-terminal halves of the NFκB subfamily proteins have ankyrin repeats-containing inhibitory domains, which can be removed by proteasome-mediated proteolysis. Like the C-terminal domains of the NFκB proteins, the independent IκB proteins consist mainly of ankyrin repeats.

signals, including cytokines, infectious agents, and radiation-induced DNA double-strand breaks,<sup>14</sup> IκB is degraded, the NFκB NLS is exposed, and NFκB undergoes nuclear uptake and becomes an active transcription factor.<sup>13</sup> IκB contains six ankyrin repeats and binds two sites in NFκB, termed here the “N site” and “C site” according to their position in NFκB<sub>p65</sub> sequence. The N site encompasses NFκB<sub>p65</sub> residues 235–245 (numbering by PDB:1nfi,<sup>15</sup> chain A); the C site encompasses NFκB<sub>p65</sub> residues 290–313 and contains the nuclear localization signal (residues 301–304) that is masked by IκB. When aberrantly regulated, NFκB is constitutively active, a phenomenon observed in various malignancies including Hodgkin’s and B-cell lymphomas, acute lymphoblastic leukemia, multiple myeloma, and breast, prostate, ovarian, lung, colon, and renal cell carcinoma (reviewed in Refs. 16 and 17).

The interaction between NFκB and ASPP2 was initially discovered using yeast two-hybrid system.<sup>12</sup> Cotransfection of 53BP2 with an NFκB<sub>p65</sub> expression plasmid, or activation of NFκB, inhibited 53BP2-induced cell death.<sup>12,18</sup> Another ASPP family member, iASPP, was found to bind and inhibit NFκB<sub>p65</sub>.<sup>19</sup> However, the precise mechanism by which these interactions affect apoptosis is yet unclear. Moreover, there are no details regarding the ASPP - NFκB<sub>p65</sub> interactions at the structural, molecular, and quantitative levels. We have recently used peptide-

based methods to identify the ASPP2<sub>ANK-SH3</sub> binding sites in NFκB<sub>p65</sub>.<sup>5</sup> Examination of the surface suggested by these peptides reveals a similarity to the binding surface of NFκB<sub>p65</sub> to its inhibitor, IκB (see Fig. 2). This similarity in the binding sites, together with the fact that both ASPP2<sub>ANK-SH3</sub> and IκB contain ankyrin repeats, led us to test whether the two proteins bind NFκB<sub>p65</sub> in a similar manner. We performed a computational study using protein docking and molecular dynamics to suggest a model for the complex of ASPP2<sub>ANK-SH3</sub> and NFκB<sub>p65</sub>. Our results show that NFκB<sub>p65</sub> binds ASPP2<sub>ANK-SH3</sub> and IκB in a similar manner, suggesting that ASPP2<sub>ANK-SH3</sub> may act as an IκB-like NFκB inhibitor.

## METHODS

### PDB structures

For NFκB, we used the X-ray structures of p50 and p65, solved in complex with IκB at 2.7 Å resolution (PDB code: 1nfi, chains A,B)<sup>15</sup>; For IκB we used its structure from the same X-ray structure (PDB: 1nfi, chain F); For ASPP2<sub>ANK-SH3</sub>, we used the p53 bound X-ray structure solved at 2.2 Å resolution (PDB code: 1ycs).<sup>6</sup> All figures were created using PyMol.<sup>20</sup>

### Hinge movement prediction

We submitted the structure of NFκB<sub>p65</sub> for hinge prediction by the HingeProt<sup>21</sup> and ElNemo<sup>22</sup> algorithms. HingeProt employs Elastic Network (EN) models, both Gaussian

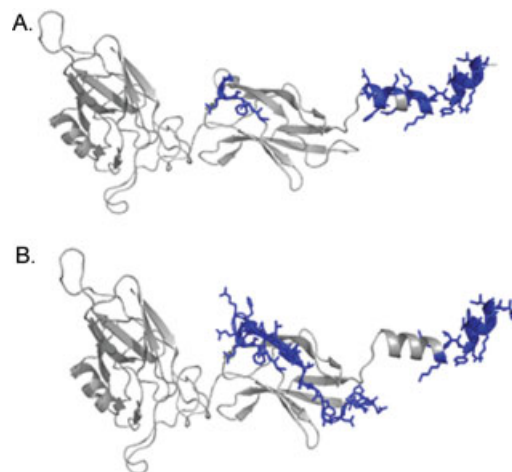


**Figure 2**

Similarity in the ASPP2<sub>ANK-SH3</sub> and IκB binding sites on NFκB<sub>p65</sub>. **A:** Gray: NFκB<sub>p65</sub>. Residues that bind IκB according to the crystal structure<sup>15</sup> are colored blue and depicted in sticks. **B:** Gray: NFκB<sub>p65</sub>. Residues that bind ASPP2<sub>ANK-SH3</sub> according to peptide array<sup>5</sup> are colored blue and depicted in sticks. Stretches of residues from NFκB<sub>p65</sub> that bind IκB are 238–245 and 294–314. According to our peptide array studies, the ASPP2<sub>ANK-SH3</sub>-binding residues of NFκB<sub>p65</sub> are 238–265 and 303–350 (<sup>5</sup> the structure is determined only until residue 314).

Network Model (GNM) and Anisotropic Network models (ANM) (detailed in Ref. 21). Given an input protein chain, HingeProt identifies the rigid parts and the hinges connecting them, and the direction of the fluctuation of each residue in the slowest two modes. Elnemo webserver is also based on Elastic Network models. It computes the low frequency normal modes of a protein and performs an extensive analysis of the predicted motion.

### Rigid docking

We used the PatchDock algorithm<sup>23</sup> to suggest a rigid docking model of NFκB<sub>p65</sub> with ASPP2<sub>ANK-SH3</sub>. Given two molecules, PatchDock computes the three-dimensional transformations of one of the molecules with respect to the other with the goal of maximizing surface shape complementarity while minimizing the number of steric clashes. For the NFκB-ASPP2<sub>ANK-SH3</sub> interaction, one molecule partner was NFκB<sub>p65</sub>, with ASPP2<sub>ANK-SH3</sub> in an aligned orientation with IκB, such that the two C-terminal ankyrin repeats of the two proteins are aligned. The other protein partner was the segment of C-terminal residues (291–314) of NFκB<sub>p65</sub>, in the IκB-bound conformation. Distance constraint between residues 290 and 291 of NFκB was introduced in order to keep the protein connected.

### Refinement

For refinement and scoring of the PatchDock results we used the FireDock algorithm.<sup>24</sup> Given a set of transformations, FireDock refines and scores the candidate models according to an energy function. Each candidate is refined by optimization of side-chain conformations and rigid-body orientation. The side-chain flexibility is modeled by rotamers and the obtained combinatorial optimization problem is solved by integer linear programming.<sup>25</sup> Following rearrangement of the side-chains, the relative position of the docking partners is refined by Monte Carlo minimization of the scoring function. The refined candidates are ranked by an energy-based score. This score includes atomic contact energy,<sup>26</sup> softened van der Waals interactions, electrostatics, H-bonding, and additional estimations of the binding free energy.

### MD simulations

The first two initial conformations comprised NFκB p50 and p65, and ASPP2<sub>ANK-SH3</sub> with their structures as determined by X-ray crystallography. ASPP2<sub>ANK-SH3</sub> was aligned to IκB: In the first conformation, ASPP2<sub>ANK-SH3</sub> ankyrin repeats were aligned to the C-terminus of IκB (repeats 3–6). In the second conformation ASPP2<sub>ANK-SH3</sub> ankyrin repeats were aligned to the N-terminus of IκB (repeats 1–4). The third starting conformation was generated using the aligned position of ASPP2<sub>ANK-SH3</sub> as in the first conformation, but with a hinge movement of the 291–314 C-terminal tail of NFκB. The hinge movement

was obtained using the HingeProt server on NFκB<sub>p65</sub>. Three rigid parts were found in the molecule, from residues 20–187, 188–291, and 292–314. Residue 291 was picked as the hinge residue. A few models of the hinge rotations were examined, the transformation in which the C-terminal tail was the closest to the location of ASPP2<sub>ANK-SH3</sub> was chosen. The HingeProt server returns the C $\alpha$  backbone atoms of the protein, thus we applied the hinge to the full atom model by performing a simple alignment between the two NFκB structures and rotation of the C-terminal tail according to the hinge that was predicted. The initial conformations are depicted in Figure 6.

### MD Procedure

The simulations were conducted using version 3.3.1 of the GROMACS MD simulation package<sup>27,28</sup> employing the GROMOS96 53a6 force-field.<sup>29</sup> The protein complex was composed from 6133 atoms in total. It was embedded in a box solvated in 33914 water molecules using the SPC model.<sup>30</sup> To neutralize the system at a physiological salt concentration of 0.1M, 99 Na<sup>+</sup> and 67 Cl<sup>-</sup> ions were added at random positions in the solvent. Thus, the entire system was composed of 107,565 atoms in total. Each system underwent energy-minimization (EM) relaxation with a tolerance of 200 KJ/mol \* nm<sup>2</sup>. Following the EM stage, the system was subjected to a positional restraints (PR) procedure for 500 ps in order to dynamically solvate the protein within the water. The protein atoms were restrained at this stage by a harmonic constraint with a force constant of  $k = 1000$  KJ/mol \* nm. Following the PR process, each of systems was subjected to a 13-ns MD simulation. As exemplified in Figure 8, the simulated complexes were very stable and reached equilibrium within a few nanoseconds, justifying the 13-ns duration. During the MD runs, the LINCS algorithm<sup>31</sup> was used to constrain the bond length of hydrogen atoms, allowing for an integration time step of 2 fs. Constraining only hydrogen related bonds in a 2 fs time step was used since it is a common procedure in such calculations (see for example Ref. 32). The simulations were conducted in the NPT ensemble, with a constant temperature of 300 K and a pressure of 1 bar. The solvent and the protein were separately coupled to Berendsen temperature bath with a coupling constant of 0.1 ps, and an isotropic pressure bath<sup>33</sup> with a coupling constant of 0.5 ps. Van der Waals (VdW) interactions were treated by using a cutoff of 12 Å. Long-range electrostatic forces were treated by using the PME algorithm.<sup>34</sup>

## RESULTS

### The ASPP2<sub>ANK-SH3</sub>-binding sites in NFκB<sub>p65</sub> reveal similarity to the IκB binding site

We have recently discovered the ASPP2<sub>ANK-SH3</sub> binding peptides from NFκB<sub>p65</sub> using peptide array screening.<sup>5</sup>

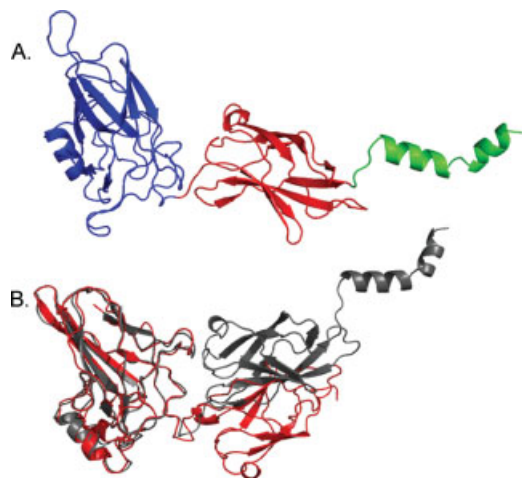


**Figure 3**

Hinge motions in NFκB<sub>p65</sub>. **A:** Hinge predictions for NFκB<sub>p65</sub> are based on the servers HingeProt<sup>21</sup> and Elnemo.<sup>22</sup> The structure of NFκB<sub>p65</sub> is colored according to the separate rigid regions. Blue: residues 20–188; Red: residues 189–290; Green: residues 290–314. **B:** Structure alignment of DNA-bound NFκB<sub>p65</sub> (PDB: 1vix, colored red) and IκB-bound NFκB<sub>p65</sub> (PDB: 1nfi, in grey). The movement is of the first two rigid parts (20–188 and 189–290) relative to each other.

The recombinant ASPP2<sub>ANK-SH3</sub> protein bound NFκB<sub>p65</sub> peptides with the following residue stretches (numbering according to PDB: 1nfi<sup>15</sup>): 21–40, 26–50, 303–329, 314–332, 330–355 and to a lesser extent 238–265 (see Fig. 2). Fluorescence anisotropy studies with the N- and C-terminal peptides showed that ASPP2<sub>ANK-SH3</sub> bound NFκB<sub>p65</sub> 303–332 with submicromolar affinity.<sup>5</sup> A visual examination of the binding peptides location on the three-dimensional structure of NFκB<sub>p65</sub> revealed a similarity between the binding surfaces of NFκB<sub>p65</sub> to ASPP2 and to its inhibitor IκB (see Fig. 2). This, in addition to the fact that both ASPP2<sub>ANK-SH3</sub> and IκB contain ankyrin repeats, raised the possibility that the two proteins bind NFκB<sub>p65</sub> in a similar manner. For such a IκB-like interaction between ASPP2<sub>ANK-SH3</sub> and NFκB to occur, two conditions are required: (i) IκB contains six ankyrin repeats, while ASPP2 contains only four. Thus, NFκB<sub>p65</sub> should undergo a backbone motion to accommodate the shorter ASPP2<sub>ANK-SH3</sub>; (ii) the suggested binding surfaces on ASPP2 should display similarity in their NFκB<sub>p65</sub>-binding features to their homologous sites on IκB. We have tested whether these two conditions are fulfilled, as described below.

### Backbone motion of NFκB<sub>p65</sub>

To check the possibility of backbone motion of NFκB<sub>p65</sub>, we submitted the structure of NFκB<sub>p65</sub> to two hinge detection servers, HingeProt<sup>21</sup> and Elnemo.<sup>22</sup> Both prediction algorithms results suggested two main

motions [Fig. 3(a)]: (i) between the first and the second domains of NFκB<sub>p65</sub>, (AA 20–190 and 191–290, respectively) (ii) motion of the C-terminal helical tail starting after residue 290. Such movements may enable NFκB<sub>p65</sub> to accommodate ASPP2<sub>ANK-SH3</sub>. We also examined the solved structures of the protein in the PDB. The first predicted domain motion is observed upon DNA binding and may be seen for example by a superposition of the solved structures of the complexes of NFκB<sub>p65</sub> with IκB (PDB: 1nfi<sup>15</sup>) and NFκB<sub>p65</sub> with DNA [PDB: 1vix,<sup>35</sup> Fig. 3(b)]. This motion is observed in all DNA-bound NFκB structures.

### Common surface-residue features between the NFκB-binding sites in IκB and ASPP2<sub>ANK-SH3</sub>

We compared the structures and sequences of ASPP2<sub>ANK-SH3</sub> and IκB, in particular the suggested (ASPP2<sub>ANK-SH3</sub>) and known (IκB) binding sites to NFκB. ASPP2<sub>ANK-SH3</sub> contains four repeats whereas IκB contains six repeats. However, only four repeats in IκB, the two N-terminal and two C-terminal repeats, contribute to the interaction with NFκB. We tested whether these sites have common features with the four ankyrin repeats of ASPP2<sub>ANK-SH3</sub>, by aligning ASPP2<sub>ANK-SH3</sub> and IκB and looking at the aligned known and suggested binding sites.

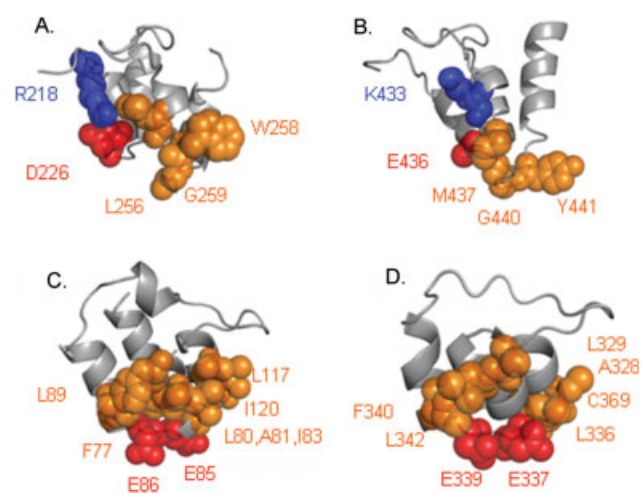


**Figure 4**

Similarity of the NFκB<sub>p65</sub> binding sites in ASPP2<sub>ANK-SH3</sub> and IκB. The suggested interaction sites of ASPP2<sub>ANK-SH3</sub> with NFκB<sub>p65</sub> are compared with the known binding sites of IκB. Hydrophobic residues are colored orange, positive in blue, and negative in red. **A:** IκB binding site to NFκB<sub>p65</sub> N-site, according to the crystal structure. **B:** ASPP2<sub>ANK-SH3</sub> putative binding site to NFκB<sub>p65</sub> N-site. Both IκB and NFκB display corresponding positive, negative, and hydrophobic residues. **C:** IκB binding site to NFκB<sub>p65</sub> C-site, according to the crystal structure. **D:** ASPP2<sub>ANK-SH3</sub> suggested binding site to NFκB<sub>p65</sub> C-site. Both IκB and ASPP2 display corresponding hydrophobic and negative residues (See text for residue details).

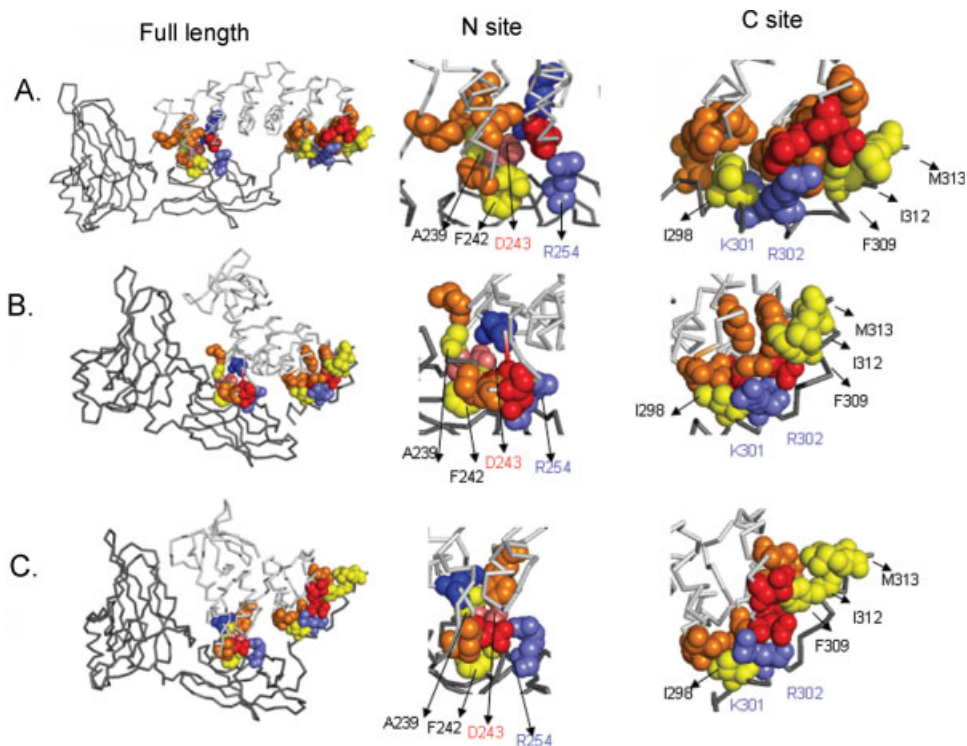


**Figure 5**

Structural models of the NFκB-ASPP2<sub>ANK-SH3</sub> complex compared with the NFκB-IκB complex. The docking model and the final conformation of molecular dynamics simulation (third initial conformation) interactions are compared with the crystal structure of NFκB-IκB complex. In all cases, NFκB<sub>p65</sub> is colored dark gray, IκB/ASPP2<sub>ANK-SH3</sub> are colored light gray. Representative binding residues, that are common to the NFκB-IκB complex and both structural models, are depicted in spheres and color coded. On NFκB, hydrophobic or aromatic residues are colored in yellow, positive in light blue, and negative in pink. On either IκB or ASPP2, hydrophobic or aromatic residues are in orange, positive in red and negative in blue. Horizontal view: **A**: The determined structure of the complex NFκB-IκB (PDB: 1nfi); **B**: Rigid docking model; **C**: Final model derived from molecular dynamics simulations of the putative NFκB-ASPP2<sub>ANK-SH3</sub> complex. A vertical view of the figure: left: full length proteins; middle: zoom in on N-site interactions; right: zoom in on C-site interactions. The full list of interactions is detailed in Table II.

The N site refers to NFκB<sub>p65</sub> residues 236–253; The C site refers to NFκB<sub>p65</sub> residues 293–313. For testing the N-site, ASPP2<sub>ANK-SH3</sub> ankyrin repeats were aligned to the C-terminus of IκB (repeats 3–6). For the C site, ASPP2<sub>ANK-SH3</sub> ankyrin repeats were aligned to the N-terminus of IκB (repeats 1–4). The ankyrin repeats comprising both the N and C site share patterns of hydrophobic, aromatic, and electrostatic residues over the two binding patches, as seen in the determined protein structures (see Fig. 4). The N-site binding surface of NFκB<sub>p65</sub> interacts with the 5th and 6th ankyrin repeats of IκB. The corresponding surface on ASPP2<sub>ANK-SH3</sub> is likely to be contributed by the 3rd and 4th ankyrin repeats. At this site, similar hydrophobic and charged residues are found [Fig. 4(a,b)]. Hydrophobic or aromatic residues of IκB at the N site are Leu256, Gly259, and Trp258. Corresponding hydrophobic or aromatic residues of ASPP2 are Met437, Gly440, and Tyr441. Charged residues of IκB at the N site are Arg218 and Asp226. The corresponding charged residues in ASPP2 are Lys433 and Glu436. The NFκB<sub>p65</sub> C-

terminal interaction site (“C-site”) containing the NLS, interacts with the two N-terminal ankyrin repeats of IκB that mask the NLS, inhibiting NFκB nuclear uptake and trans-activation activity.<sup>15</sup> Within the first and second repeats, IκB binds NFκB via two continuous sequences: residues 72–89 and 117–122. The similarity of features between IκB and ASPP2<sub>ANK-SH3</sub> is observed in both stretches of residues: A cluster of hydrophobic residues and a pair of negatively charged residues are found in both proteins [Fig. 4(c,d)]. In the C site of IκB, hydrophobic or aromatic residues consist of Phe77, Leu80, Ala81, Ile83, Leu89, Ile120, and Leu117. In the suggested C site of ASPP2<sub>ANK-SH3</sub>, Ala328, Leu329, Leu336, Phe340, Leu342, and Cys369 may contribute the corresponding hydrophobic and aromatic properties. The residue pair Glu85–Glu86 of IκB binds the NLS of NFκB<sub>p65</sub>. Possible corresponding contribution may be given by ASPP2 residues Glu337 and Glu339. In summary, IκB and ASPP2<sub>ANK-SH3</sub> have common binding properties and thus may bind in a similar manner to NFκB.

**Table I**Comparison of the Interacting Residue Pairs in the NFκB-IκB Complex and in the NFκB-ASPP2 Complex Models<sup>a</sup>

NFκB	IκB (solved structure, <sup>15</sup> )	ASPP2 (docking)	ASPP2 (MD)	Site <sup>b</sup>	Type <sup>c</sup>
R236		E436,E438,E439	E435,E436,E438	N	E
G237		M437	M437	N	H
<b>F239</b>	<b>G259</b>	<b>M437</b>	<b>M437</b>	<b>N</b>	<b>H</b>
<b>A242</b>	<b>Y251,L256,M279</b>	<b>M427</b>	<b>W394</b>	<b>N</b>	<b>H</b>
<b>D243</b>	<b>R218</b>	<b>K433</b>	<b>K433</b>	<b>N</b>	<b>E</b>
H245		D426	D392,W394,D426	N	E
R246	E282		D426	N	E
<b>R253</b>	<b>D226</b>	<b>E435,E436,E439</b>	<b>E436</b>	<b>N</b>	<b>E</b>
D293	R143				
D294	R143				
R297		D333,E337			
R297		E337	E337	C	E
<b>I298</b>	<b>I83,L110,L117,I120</b>	<b>L336,G338,A370</b>	<b>L336,C369,A370,G371</b>	<b>C</b>	<b>H</b>
<b>K301</b>	<b>D73, D75</b>	<b>D333,E337,E339</b>	<b>D333,E337,E359</b>	<b>C</b>	<b>E</b>
<b>R302</b>	<b>E85, E86</b>	<b>E337,E339</b>	<b>E337,E339</b>	<b>C</b>	<b>E</b>
R304	E72,D73	E337, E339	E333	C	E
Y306	H84			C	A
<b>F309</b>	<b>F77,L80,A81,H84,L89</b>	<b>G338,F340,I375</b>	<b>L330, L342</b>	<b>C</b>	<b>H</b>
<b>I312</b>	<b>F77, L80</b>	<b>F340</b>	<b>L330, L342</b>	<b>C</b>	<b>H</b>
<b>M313</b>	<b>F77</b>	<b>F340</b>	<b>L342</b>	<b>C</b>	<b>H</b>

<sup>a</sup>The table details the residue pairs that interact in the experimentally solved NFκB-IκB complex,<sup>15</sup> the selected rigid docking model and the stabilized conformation resulting from molecular dynamics simulations (third starting orientation). The table shows the residues from IκB or ASPP2<sub>ANK-SH3</sub> that interact with residues from NFκB. The residue interactions of ASPP2 are derived from the structural models of ASPP2<sub>ANK-SH3</sub>-NFκB obtained by rigid docking and MD simulations. Residue interactions that are common in the complex models and in the NFκB-IκB complex are bolded.

<sup>b</sup>N site refers to residues 235–245 of NFκB. C site refers to residues 290–313 of NFκB.

<sup>c</sup>Interaction type, E, electrostatic; H, hydrophobic; A, aromatic.

### Rigid docking suggests a model for the NFκB<sub>p65</sub> · ASPP2<sub>ANK-SH3</sub> complex, which is similar to the NFκB-IκB complex

We applied rigid docking<sup>23</sup> followed by model refinement<sup>24</sup> to construct a structural model for the complex between NFκB<sub>p65</sub> and ASPP2<sub>ANK-SH3</sub>. The 3rd ranked solution out of 68 generated solutions was in agreement with the experimental peptide binding data, that is,

involves binding of NFκB<sub>p65</sub> peptides 238–265 and 303–313. This model suggested a structure that resembles many of the NFκB-IκB residue-residue interactions [Fig. 5(b), Table I]. In particular, the positively charged NLS residues 301, 302, and 304 are within interaction distance from ASPP2 residues Glu337 and Glu339, which correspond to IκB residues Glu85 and Glu86 that mask the NFκB<sub>p65</sub> NLS. Assessment of the model using the Coilcheck<sup>36</sup> and FastContact<sup>37</sup> algorithms suggests that the model has a low energy, comparable with the energy assessment of the interaction between IκB (PDB: 1nfi, chain F) and NFκB (PDB: 1nfi, chain A). The results are summarized in Table II. The rigid docking, even when followed by refinement, is incapable of predicting protein motions in solution. Rather, it provides a low resolution, rough assessment of geometrically and chemically complementary surfaces. To assess the stability and behavior of the complex in solution we subjected the complex to molecular dynamics simulations.

**Table II**Energy Assessment of the NFκB-ASPP2 Structural Models<sup>a</sup>

<b>FastContact<sup>37</sup></b>	<b>PDB:1nfi<sup>15</sup></b>	<b>Docking</b>	<b>MD</b>
Electrostatic (4r) Energy (kcal/mol)	−47.96	−42.80	−50.2
Desolvation Free Energy (kcal/mol)	13.23	12.57	12.8
van der Waals (CHARMm19, kcal/mol)	−2715	−2707	−2610
<b>CoilCheck<sup>36</sup></b>	<b>PDB:1nfi<sup>15</sup></b>	<b>Docking</b>	<b>MD</b>
Total Stabilizing Energy (kJ/mol)	−352.73	−112.54	−179.9
van der Waals Energy (kJ/mol)	−185.86	−62.08	−180.9
Energy per Residue (kJ/mol)	−0.69	−0.22	−0.37
No. of van der Waals Pairs	2771	1480	4959
No. Potential Favorable Electrostatic Interactions	71	35	64

<sup>a</sup>The docking model and the stabilized conformation resulting from molecular dynamics simulation (third starting orientation) were submitted for energy assessment by two algorithms: Coilcheck<sup>36</sup> and FastContact<sup>37</sup>. The values were compared with those of the interaction between NFκB and IκB, according to the crystal structure. The table shows that the energy assessment of the ASPP2<sub>ANK-SH3</sub>-NFκB modeled structures is similar to the assessment of the experimentally determined complex of NFκB and IκB.

### Molecular dynamics simulations of the putative ASPP2<sub>ANK-SH3</sub> · NFκB complex, support an interaction that is similar to IκB

We used molecular dynamics simulations to assess the stability and dynamics of the interactions in the proposed ASPP2<sub>ANK-SH3</sub>-NFκB complex. We tested whether an ASPP2<sub>ANK-SH3</sub>-NFκB<sub>p65</sub> complex will stay in contact or dissociate in solution and examined protein motion and interaction details during the simulation. Since

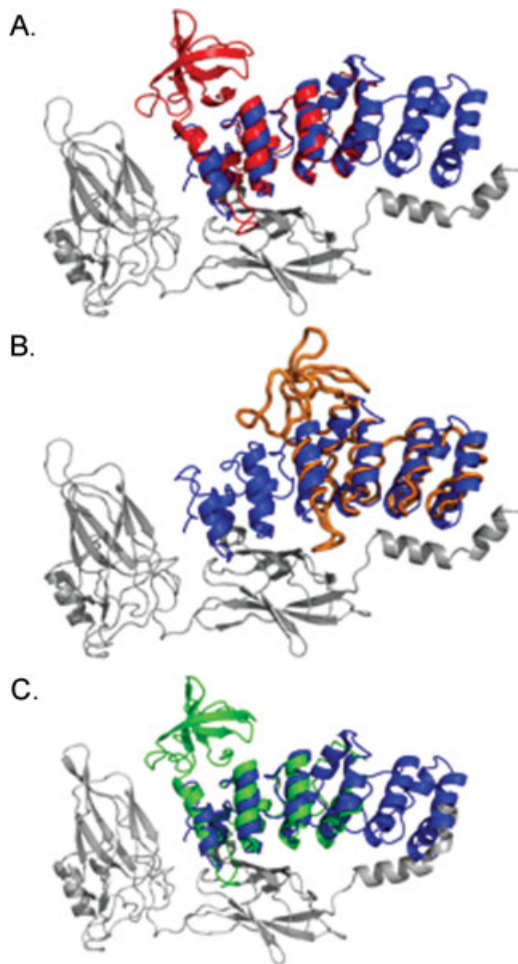


**Figure 6**

Molecular dynamics initial conformations with different positions of ASPP2<sub>ANK-SH3</sub>. **A–C:** In grey, NFκB<sub>p65</sub>, in blue, IκB. **A:** In red, ASPP2<sub>ANK-SH3</sub> aligned to IκB. The C terminal repeats are aligned. **B:** In orange, ASPP2<sub>ANK-SH3</sub> aligned to IκB. The N terminal repeats are aligned. **C:** In green, ASPP2<sub>ANK-SH3</sub> aligned to IκB. The C terminal repeats are aligned. NFκB<sub>p65</sub> C-terminal tail is slightly hinge-bent according to HingeProt<sup>21</sup> prediction.

ASPP2 has only four ankyrin repeats and IκB has six, we used three different initial structures for the MD simulations (see Fig. 6). In conformations 1 and 2, NFκB<sub>p65</sub> and p50 coordinates were taken from the solved structure in complex with IκB. The starting position of ASPP2<sub>ANK-SH3</sub> was based on a structural alignment to IκB: In the first orientation, the C termini of ASPP2<sub>ANK-SH3</sub> and IκB ankyrin repeats are aligned [Fig. 6(a)]; in the second orientation, the N termini of ASPP2<sub>ANK-SH3</sub> and IκB are aligned [Fig. 6(b)]. In the third conformation, the position of ASPP2 was the same as in the first conformation, but with an added hinge transformation on NFκB<sub>p65</sub> as predicted by the HingeProt algorithm.<sup>21</sup> Simulations were run for 13 ns and the system behavior in each case is described below. The interaction distance threshold

was 6 Å and 8 Å for hydrophobic and electrostatic interactions, respectively. We measured the distances of 17 residue pairs, 7 pairs from the N site and 10 pairs from the C site. These putative interactions were selected based on the similar positions of the binding residues in IκB and ASPP2<sub>ANK-SH3</sub>. The examined residue pairs (first residue from NFκB<sub>p65</sub>, second from ASPP2<sub>ANK-SH3</sub>) for the N site were: G237-M437; F239-M437; R236-E436; R236-E439; D243-K433; H245-D426; R253-E436. For the C site, I298-L336; I298-A370; K301-D333; R302-E307; I312-L330; I312-L342; M313-L330, M313-L342; F309-L330; F309-L342.

In the first two conformations, where only one binding site was in interaction at the initial structure, observations were: (i) the system stayed stable throughout the simulation, that is, the two proteins remained in contact and each kept a stable structure that hardly changed during the simulation; (ii) the binding site that was in interaction in the initial conformation (N site in the first conformation and C site in the second conformation) remained in interaction during the simulation. The binding site that was not in interaction in the initial conformation (C site for the first conformation and N site for the second conformation) did not form an interaction during the simulation.

We suspected that the reason for not forming interactions in both binding sites in the first two simulations is that in each of the initial structures, one pair of binding site surfaces is too far in space to form interactions. It could be that the water provides masking of the partial charges on each site, so that each surface does not affect the other to create a local movement that will bring them closer together. Thus, we ran the third simulation, in which the starting conformation is the same as conformation 1, but in addition we applied a moderate hinge transformation on NFκB<sub>p65</sub> as described in the Materials and Methods section and in Figure 6(c). This was done to decrease the distance between the predicted C-site surfaces of NFκB<sub>p65</sub> and ASPP2. Still, the distances between predicted C-site residue pairs in the beginning of the simulation are large (average of  $12.4 \pm 2$  Å) but smaller than in conformation 1 (average of  $18.1 \pm 3.6$  Å). Here, despite that only the N-site started in contact in the initial structure as in conformation 1, the structures relax into a state where both binding sites got to be within interaction distance most of the simulation. Sixteen out of 17 predicted interactions are formed and maintained during the simulation. The exception was the residue pair I312-L342. Furthermore, the C-terminal helical tail is undergoing additional hinge bending motion. The process may be seen from a view of the initial and final coordinates of NFκB<sub>p65</sub> in the simulation [Fig. 7(a)]. A representative distance plot during the simulation between residues R302 (NFκB<sub>p65</sub>) and E337 (ASPP2) reflects this process [Fig. 7(b)]. The representative residue interactions are depicted in Figure 5(c).

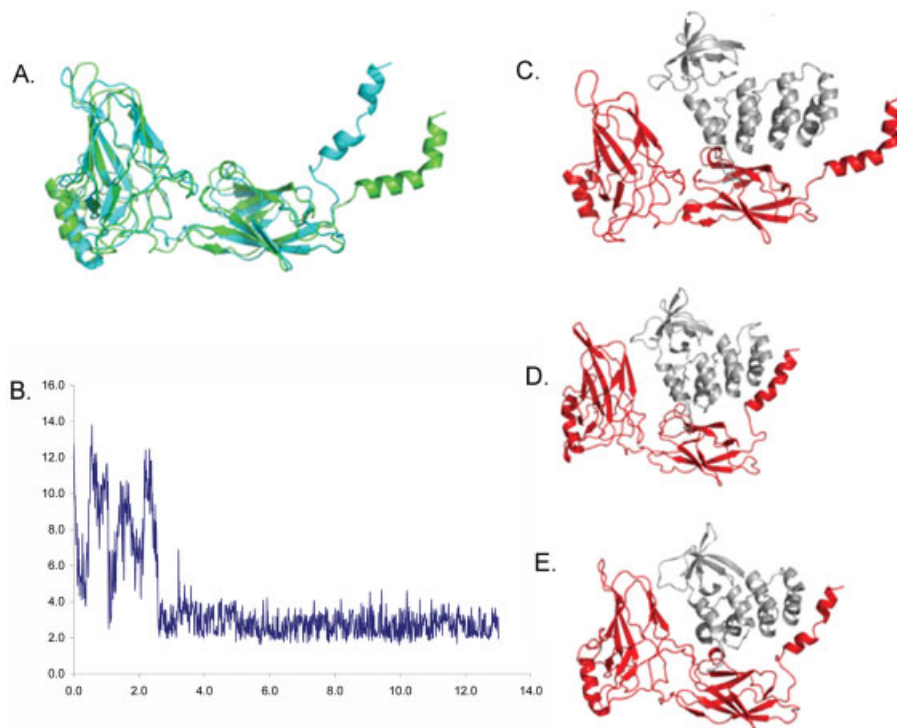


**Figure 7**

Molecular dynamics of the NFκB-ASPP2<sub>ANK-SH3</sub> complex. **A:** In cyan, initial conformation of NFκB in the simulation; in green, the final conformation of NFκB<sub>p65</sub> in the simulation. **B:** The distance between NFκB NLS residue Arg302 and ASPP2 Glu337 during the simulation. Y axis: distance in angstroms; X axis: time (ns). **C–E:** Snapshots of NFκB<sub>p65</sub> and ASPP2<sub>ANK-SH3</sub> during the simulation of the third conformation [Fig. 6(C)] at time 0 (C), after 6 ns (D) and at the end of simulation, 13 ns (E). NFκB<sub>p65</sub> is colored red, ASPP2<sub>ANK-SH3</sub> is colored gray.

Root Mean Square Deviation (RMSD) was used to examine the stability and the convergence of the proteins during the dynamics. All protein chains seem to converge after ~4 ns of simulation, and maintain a stable conformation from there and after (see Fig. 8). The main movement in NFκB<sub>p65</sub> during simulation is of the C-terminal tail (residues 290–313), as may be seen from the comparison of RMSD of NFκB<sub>p65</sub> with and without its C-terminal tail. Although NFκB<sub>p65</sub> residues 20–290 had a rather low RMSD (4 Å), the full length chain NFκB<sub>p65</sub> displays significant movement relative to the initial conformation, between 6 and 8 Å (black and red lines in Fig. 8, respectively). In addition, ASPP2<sub>ANK-SH3</sub> and NFκB<sub>p50</sub> chains maintain a stable and low RMSD throughout the simulation. 2 Å for the NFκB<sub>p50</sub> chain and 4 Å for ASPP2<sub>ANK-SH3</sub>.

It appears that the additional hinge bending motion has facilitated the formation of the C-site interactions through which ASPP2 may block the NFκB NLS in a similar manner to IκB. The final conformation was submitted to the energy assessment servers FastContact<sup>37</sup> and CoilCheck<sup>36</sup> (Table II). The final conformation is assessed as having low energy, comparable with the values of the complex NFκB-IκB.

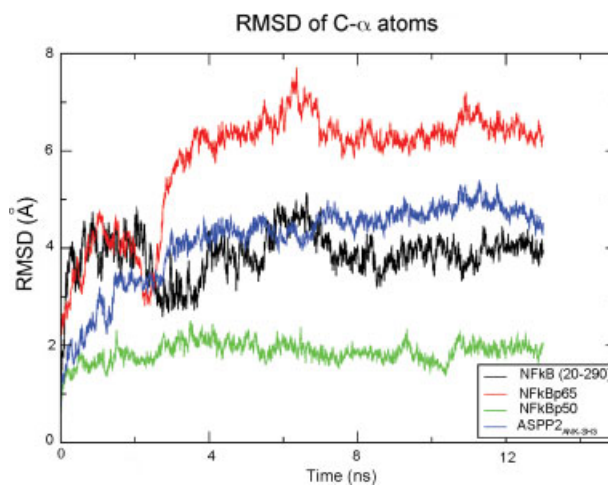


**Figure 8**

Root mean square deviations (RMSD) of protein chains during MD simulation. The graph depicts the movement of the protein chains during the simulation of the third conformation. In green, NFκB chain p50, blue: ASPP2<sub>ANK-SH3</sub>, black: NFκB<sub>p65</sub> residues 20–290, red: NFκB<sub>p65</sub>. The main contribution to chain movement of NFκB<sub>p65</sub> comes from the C-terminal tail, residues 290–313.

## DISCUSSION

In this study, we analyzed the interaction between ASPP2<sub>ANK-SH3</sub> and NFκB<sub>p65</sub>. Since the binding site of NFκB to ASPP2<sub>ANK-SH3</sub> is similar to the binding site with its inhibitor IκB,<sup>5</sup> we checked the possibility that ASPP2<sub>ANK-SH3</sub> binds NFκB in a similar manner and thus may function as an NFκB inhibitor. Our results show that the NFκB-binding properties of ASPP2<sub>ANK-SH3</sub> and IκB are similar, and that NFκB<sub>p65</sub> is likely to undergo hinge movement that may facilitate ASPP2 binding. We also performed a rigid docking between the NFκB<sub>p65</sub> C-terminal tail and the rest of the structure while in complex with ASPP2. The third ranked solution displays many of the interactions predicted by structure-based comparison to IκB. Last, we carried out molecular dynamics simulations of the putative NFκB-ASPP2<sub>ANK-SH3</sub> complex in three starting orientations, of which one displayed a stable interaction in both predicted binding sites.

### NFκB binding by ASPP2<sub>ANK-SH3</sub> and IκB is similar

The determined structures of NFκB in the PDB as well as flexibility prediction by two independent servers suggest backbone flexibility in NFκB<sub>p65</sub>. As ASPP2 contains four ankyrin repeats while IκB contains six repeats, such flexibility may facilitate the predicted interaction between NFκB and ASPP2<sub>ANK-SH3</sub> by enabling NFκB<sub>p65</sub> to accommodate the shorter ASPP2<sub>ANK-SH3</sub>. An examination of the binding properties of IκB and ASPP2 revealed that the proteins share similar patterns of binding properties at the N- and C- binding sites. At the N-site, a hydrophobic cluster, one positive and one negative residue; at the C-site, clusters of hydrophobic and negatively charged residues (see Fig. 4). The C site is in particular important as it contains the core of NFκB inhibition by IκB: binding of the positively charged nuclear localization signal (AA 301-304). Such binding by ASPP2 may serve as an alternative mechanism to inhibit NFκB and prevent its constitutive activation and therefore promote apoptosis in malignant cells.

The final conformation in the MD simulation and the docking solution, though not fully identical, have some common residue-residue interactions at the N and C sites. At the N sites, both models point at Lys433, Glu436, and Met437 from ASPP2<sub>ANK-SH3</sub> as binding Asp243, Arg253, and Phe239 of NFκB<sub>p65</sub>. At the C site, both models suggest interactions between the positively charged NFκB NLS and negatively charged residues in ASPP2<sub>ANK-SH3</sub>, in particular residues Glu337 and Glu339 from ASPP2<sub>ANK-SH3</sub>, with residues Lys301-Arg302 from NFκB<sub>p65</sub> (Table II). These interactions are part of the inhibitory mechanism of NFκB by IκB and may be the mechanism for NFκB inhibition by ASPP2. In a similar

study, Latzer *et al.*<sup>38</sup> used associative memory Hamiltonian (AMH) to simulate the NLS-containing parts of NFκB p50 and p65, in the free and bound states with IκBα and IκBβ. We observed several similarities between the simulation of the NFκB<sub>p65</sub>-IκBα interaction and our simulation of the NFκB<sub>p65</sub>-ASPP2<sub>ANK-SH3</sub> interaction: (i) In both cases, the NLS-containing polypeptide tends to be unstable but acquires a structure upon binding the protein ligand; (ii) In both cases, the NLS-containing polypeptide acquires a split-helical conformation; (iii) In both cases, the NLS location is at the bend and turn region of the polypeptide. This similarity supports our suggestion that ASPP2 may bind NFκB in a similar manner to its natural inhibitor, IκB.

Recently, we found that the proline-rich domain of ASPP2 (ASPP2<sub>Pro</sub>) binds ASPP2<sub>ANK-SH3</sub>, and competes with the C-terminal peptide of NFκB<sub>p65</sub> on ASPP2<sub>ANK-SH3</sub> binding.<sup>5</sup> ASPP2<sub>Pro</sub> bound three peptides of ASPP2<sub>ANK-SH3</sub>, two in the SH3 domain and one in the ankyrin repeats domain. The binding peptide in the ankyrin repeats domain is at the N-terminal repeat, which according to our model binds the NLS-containing NFκB C-site. Binding this peptide by ASPP2<sub>Pro</sub> may thus regulate the interaction between ASPP2<sub>ANK-SH3</sub> and NFκB<sub>p65</sub>. It was also shown that NFκB<sub>p65</sub> can bind either the SH3 or the ankyrin repeats domain.<sup>12</sup> In the MD model final conformation, there are indeed contacts between the SH3 domain and NFκB<sub>p65</sub>. We focused our analysis on the contacts that structurally correspond to the IκB-NFκB<sub>p65</sub> interaction but our MD model is also in agreement with SH3 participation in the interaction.

### ASPP2<sub>ANK-SH3</sub> as a potential IκB-like NFκB inhibitor

NFκB is a highly important transcription factor and hence is heavily regulated in cells. Normally it is maintained in the cytoplasm due to binding IκB. When free upon inhibitor release, NFκB goes to the nucleus and up-regulates antiapoptotic genes. ASPP2 is known as a stimulator of p53-mediated apoptosis. ASPP2 also interacts with Bcl-2 antiapoptotic members<sup>2,8</sup> and is likely to regulate Bcl-2-mediated apoptosis. Here we suggest a novel mechanism for the antiapoptotic function of ASPP2 by inhibiting NFκB. For example, NFκB up-regulates Bcl-X and other antiapoptotic proteins at the transcription level. Inhibiting NFκB by ASPP2 is thus a possible mechanism by which ASPP2 exerts its apoptotic activity.

## ACKNOWLEDGMENTS

We thank Dr. Dina Schneidman-Duhovny for stimulating discussions and critical review of the manuscript.

## REFERENCES

- Iwabuchi K, Bartel PL, Li B, Marraccino R, Fields S. Two cellular proteins that bind to wild-type but not mutant p53. *Proc Natl Acad Sci USA* 1994;91:6098–6102.
- Naumovski L, Cleary ML. The p53-binding protein 53BP2 also interacts with Bcl2 and impedes cell cycle progression at G2/M. *Mol Cell Biol* 1996;16:3884–3892.
- Samuels-Lev Y, O'Connor DJ, Bergamaschi D, Trigiante G, Hsieh JK, Zhong S, Campargue I, Naumovski L, Crook T, Lu X. ASPP proteins specifically stimulate the apoptotic function of p53. *Mol Cell* 2001;8:781–794.
- Tidow H, Andreeva A, Rutherford TJ, Fersht AR. Solution structure of ASPP2 N-terminal domain (N-ASPP2) reveals a ubiquitin-like fold. *J Mol Biol* 2007;371:948–958.
- Rotem S, Katz C, Benyamini H, Lebendiker M, Veprintsev D, Rudiger S, Danieli T, Friedler A. The structure and interactions of the proline-rich domain of ASPP2. *J Biol Chem* 2008;283:18990–18999.
- Gorina S, Pavletich NP. Structure of the p53 tumor suppressor bound to the ankyrin and SH3 domains of 53BP2. *Science* 1996;274:1001–1005.
- Robinson RA, Lu X, Jones EY, Siebold C. Biochemical and structural studies of ASPP proteins reveal differential binding to p53, p63, and p73. *Structure* 2008;16:259–268.
- Katz C, Benyamini H, Rotem S, Lebendiker M, Danieli T, Iosub A, Refaely H, Dines M, Bronner V, Bravman T, Shalev DE, Rudiger S, Friedler A. Molecular basis of the interaction between the antiapoptotic Bcl-2 family proteins and the proapoptotic protein ASPP2. *Proc Natl Acad Sci USA* 2008;105:12277–12282.
- Helps NR, Barker HM, Elledge SJ, Cohen PT. Protein phosphatase 1 interacts with p53BP2, a protein which binds to the tumour suppressor p53. *FEBS Lett* 1995;377:295–300.
- Espanel X, Sudol M. Yes-associated protein and p53-binding protein-2 interact through their WW and SH3 domains. *J Biol Chem* 2001;276:14514–14523.
- Cao Y, Hamada T, Matsui T, Date T, Iwabuchi K. Hepatitis C virus core protein interacts with p53-binding protein, 53BP2/Bbp/ASPP2, and inhibits p53-mediated apoptosis. *Biochem Biophys Res Commun* 2004;315:788–795.
- Yang JP, Hori M, Takahashi N, Kawabe T, Kato H, Okamoto T. NF- $\kappa$ B subunit p65 binds to 53BP2 and inhibits cell death induced by 53BP2. *Oncogene* 1999;18:5177–5186.
- Gilmore TD. Introduction to NF- $\kappa$ B: players, pathways, perspectives. *Oncogene* 2006;25:6680–6684.
- Hacker H, Karin M. Regulation and function of IKK and IKK-related kinases. *Sci STKE* 2006;2006(357):re13.
- Jacobs MD, Harrison SC. Structure of an IkappaBalpha/NF-kappaB complex. *Cell* 1998;95:749–758.
- Basseres DS, Baldwin AS. Nuclear factor-kappaB and inhibitor of kappaB kinase pathways in oncogenic initiation and progression. *Oncogene* 2006;25:6817–6830.
- Dutta J, Fan Y, Gupta N, Fan G, Gelinas C. Current insights into the regulation of programmed cell death by NF- $\kappa$ B. *Oncogene* 2006;25:6800–6816.
- Takahashi N, Kobayashi S, Kajino S, Imai K, Tomoda K, Shimizu S, Okamoto T. Inhibition of the 53BP2-mediated apoptosis by nuclear factor kappaB and Bcl-2 family proteins. *Genes Cells* 2005;10:803–811.
- Yang JP, Hori M, Sanda T, Okamoto T. Identification of a novel inhibitor of nuclear factor-kappaB. Rel A-associated inhibitor *J Biol Chem* 1999;274:15662–15670.
- Delano WL. The PyMOL molecular graphics system. San Carlos, CA: DeLano Scientific LLC; 2002. Available at: <http://www.pymol.org>.
- Emekli U, Schneidman-Duhovny D, Wolfson HJ, Nussinov R, Haliloglu T. HingeProt: automated prediction of hinges in protein structures. *Proteins* 2008;70:1219–1227. Available at: <http://bioinfo3d.cs.tau.ac.il/HingeProt/index.html>.
- Suhre K, Sanejouand YH. ElNemo: a normal mode web server for protein movement analysis and the generation of templates for molecular replacement. *Nucleic Acids Res* 2004;32(Web Server issue):W610–614. <http://www.igs.cnrs-mrs.fr/elnemo/>.
- Duhovny D, Nussinov R, Wolfson HJ. Efficient unbound docking of rigid molecules. In: Guigo R, Gusfield D, editors. Rome, Italy: LNCS; 2002. pp 185–200.
- Andrusier N, Nussinov R, Wolfson HJ. FireDock: fast interaction refinement in molecular docking. *Proteins* 2007;69:139–159.
- Kingsford CL, Chazelle B, Singh M. Solving and analyzing side-chain positioning problems using linear and integer programming. *Bioinformatics* 2005;21:1028–1036.
- Zhang C, Vasmatzis G, Cornette JL, DeLisi C. Determination of atomic desolvation energies from the structures of crystallized proteins. *J Mol Biol* 1997;267:707–726.
- Van Der Spoel D, Lindahl E, Hess B, Groenhof G, Mark AE, Berendsen HJ. Gromacs: fast, flexible, and free. *J Comput Chem* 2005;26:1701–1718.
- Lindahl E, Hess B, Van Der Spoel D. Gromacs 3.0: a package for molecular simulation and trajectory analysis. *J Mol Mod* 2001; 7:306–317.
- Oostenbrink C, Villa A, Mark AE, van Gunsteren WF. A biomolecular force field based on the free enthalpy of hydration and solvation: the GROMOS force-field parameter sets 53A5 and 53A6. *J Comput Chem* 2004;25:1656–1676.
- Berendsen HJC, Postma JPM, Van Gunsteren WF, Hermans J. Interaction models for water in relation to protein hydration. *Nature* 1969;224:175–177.
- Hess B, Bekker H, Berendsen HJC, Fraaije JGEM. LINCS: a linear constraint solver for molecular simulations. *J Comp Chem* 1997; 18:1463–1472.
- Ivanov I, Tainer JA, McCammon JA. Unraveling the three-metal-ion catalytic mechanism of the DNA repair enzyme endonuclease IV. *Proc Natl Acad Sci USA* 2007;104:1465–1470.
- Berendsen HJC, Postma JPM, Gunsteren WFV, DiNola A, Haak JR. Molecular dynamics with coupling to an external bath. *J Chem Phys* 1984;81:3684–3690.
- Essmann U, Perera L, Berkowitz ML, Darden T, Lee H, Pedersen LG. A smooth particle mesh Ewald method. *J Chem Phys* 1995; 103:8577–8593.
- Chen FE, Huang DB, Chen YQ, Ghosh G. Crystal structure of p50/p65 heterodimer of transcription factor NF- $\kappa$ B bound to DNA. *Nature* 1998;391:410–413.
- Alva V, Devi DP, Sowdhamini R. Coilcheck: an interactive server for the analysis of interface regions in coiled coils. *Protein Pept Lett* 2008;15:33–38.
- Camacho CJ, Zhang C. FastContact: rapid estimate of contact and binding free energies. *Bioinformatics* 2005;21:2534–2536.
- Latzler J, Papoian GA, Prentiss MC, Komives EA, Wolynes PG. Induced fit, folding, and recognition of the NF- $\kappa$ B-nuclear localization signals by IkappaBalpha and IkappaBbeta. *J Mol Biol* 2007;367:262–274.